1521-0111/12/8206-1074–1081$25.00
MOLECULAR PHARMACOLOGY
Vol. 82, No. 6
78998/3804600

Mol Pharmacol 82:1074–1081, 2012

Ifenprodil Effects on GluN2B-Containing Glutamate Receptors

Stacy A. Amico-Ruvio,[1] Meaghan A. Paganelli, Jason M. Myers, and Gabriela K. Popescu

Department of Biochemistry (S.A.A., J.M.M., G.K.P.) and Neuroscience Program (M.A.P., G.K.P.), School of Medicine and Biomedical Sciences, University at Buffalo, Buffalo, New York

Received March 28, 2012; accepted August 30, 2012

ABSTRACT

N-Methyl-D-aspartate (NMDA) receptors are glutamate- and glycine-gated channels that mediate fast excitatory transmission in the central nervous system and are critical to synaptic development, plasticity, and integration. They have a rich complement of modulatory sites, which represent important pharmacological targets. Ifenprodil is a well tolerated NMDA receptor inhibitor; it is selective for GluN2B-containing receptors and has neuroprotective effects. The mechanism by which ifenprodil inhibits NMDA receptor responses is not fully understood. The inhibition is incomplete and noncompetitive with other known NMDA receptor agonists or modulators, although reciprocal effects have been reported between ifenprodil potency and that of extracellular ligands including glutamate, glycine, zinc, protons, and polyamines. Recent structural studies revealed that ifenprodil binds to a unique site at the interface between the extracellular *N* termini of GluN1 and GluN2B subunits, supporting the view that interactions with other extracellular modulators are indirect. In this study, we examined how ifenprodil affects the gating reaction of NMDA receptors in conditions designed to minimize actions by contemporaneous ligands. We found that ifenprodil decreased NMDA receptor equilibrium open probability by raising an energetic barrier to activation and also by biasing the receptor toward low open probability gating modes. These results demonstrate intrinsic effects of ifenprodil on NMDA receptor stationary gating kinetics and provide means to anticipate how ifenprodil will affect receptor responses in defined physiological and pathological circumstances.

Introduction

NMDA receptors are critical to fundamental properties of the central nervous system but also contribute to several debilitating brain pathologies and dysfunctions (Cull-Candy, 2007; Kalia et al., 2008). Excessive activation of NMDA receptors has been implicated in excitotoxic neurodegeneration, and NMDA receptor inhibitors hold promise as clinically useful therapeutics. Ifenprodil, a synthetic phenylethanolamine, is the lead compound within a series of subtype-specific inhibitors that exhibit >200-fold selectivity for GluN2B (2B)-containing NMDA receptors (Carron et al., 1971; Carter et al., 1988; Williams, 1993). The specificity, high potency, and positive therapeutic index of the ifenprodil isoform generated vivid interest in defining its mechanism of action at NMDA receptors.

High-affinity ifenprodil inhibition of NMDA receptor currents occurs in the nanomolar range and is mediated through an extracellularly located binding site (Carter et al., 1988; Legendre and Westbrook, 1991). This inhibition is incomplete, does not alter single-channel conductance, and causes channel openings to become shorter and less frequent (Reynolds and Miller, 1989; Legendre and Westbrook, 1991). This evidence strongly supports an allosteric mechanism; however, whether ifenprodil has direct, intrinsic effects on channel gating or acts indirectly by modifying the receptor's sensitivity to coexisting extracellular ligands remains to be determined. Ifenprodil-bound NMDA receptors have ~5-fold higher apparent affinity for glutamate, are less sensitive to glycine, and are more sensitive to inhibition by omnipresent cations such as protons and zinc (Ransom, 1991; Kew et al., 1996; Mott et al., 1998; Rachline et al., 2005). On the basis of these observations, it was proposed that ifenprodil may lower channel open probability by reducing glycine potency (Williams, 1993), by increasing the occupancy of agonist-bound desensitized states (Kew et al., 1996), and by enhancing tonic inhibition by ambient protons (Mott et al., 1998).

NMDA receptors are obligate heterotetramers of two glycine-binding GluN1 subunits and two glutamate-binding GluN2 subunits. Four GluN2 subunits (A–D) have tightly regulated expression in vivo and determine the receptor's

This work was supported by the National Institutes of Health National Institute of Neurological Disorders and Stroke [Grant 052669].

S.A.A.-R. and M.A.P. contributed equally to this work and should be considered co-first authors.

[1] Current affiliation: Department of Neurobiology and Anatomy, School of Medicine and Dentistry, University of Rochester, Rochester, New York.

Article, publication date, and citation information can be found at http://molpharm.aspetjournals.org.
http://dx.doi.org/10.1124/mol.112.078998.

ABBREVIATIONS: NMDA, *N*-methyl-D-aspartate; 2B, GluN2B; NTD, N-terminal domain; LBD, ligand-binding domain; HEPBS, *N*-(2-hydroxyethyl) piperazine-*N*′-(4-butanesulfonic acid); IFN, ifenprodil; CTR, control; MCT, mean closed time; MOT, mean open time.

pharmacology and kinetics. The extracellular portion of each subunit consists of two structural modules: an N-terminal domain (NTD) and a ligand-binding domain (LBD), which in tetrameric receptors arrange as stacked dimers of heterodimers (Sobolevsky et al., 2009; Karakas et al., 2011; Lee and Gouaux, 2011). Structural data established in atomic detail that glycine and glutamate bind within the LBD clefts of GluN1 and GluN2 subunits, respectively (Furukawa and Gouaux, 2003; Furukawa et al., 2005; Inanobe et al., 2005), zinc binds within the NTD clefts of GluN2 subunits (Karakas et al., 2009), and ifenprodil binds to residues located deep within the dimer interface formed by GluN1 and GluN2 NTDs (Karakas et al., 2011). Residues responsible for proton inhibition have not been identified with certainty but are most likely located within the NTD of GluN1 subunits (Banke et al., 2005; Huggins and Grant, 2005). The merged structural view shows unequivocally that these modulatory sites are discrete and that they reside at considerable distance from each other; however, the picture of how they influence receptor gating and each other's actions is still incomplete.

Ample functional evidence demonstrates reciprocal influences between perturbations in the NTD and LBD layers and has consolidated the view that NTD ligands represent allosteric modulators with high therapeutic potential. Furthermore, as mathematical descriptions of single-molecule behaviors have continued to improve, detailed kinetic mechanisms for these inhibitory actions have been delineated (Banke et al., 2005; Amico-Ruvio et al., 2011). Essentially, the activation of 2B receptors consists of rapid agonist binding, slow channel gating, even slower channel desensitization, and occasional gating-mode changes. Single-channel measurements showed that after binding glutamate and before populating open states, (glycine-bound) receptors transition through at least three kinetically resolvable preopen states; occasionally, receptors escape this active gating cycle by entering desensitized states, and on a minutes time scale they can also change the gating mode (Banke and Traynelis, 2003; Amico-Ruvio and Popescu, 2010). With this model in mind, allosteric ligands may inhibit NMDA receptors by causing preopen or desensitized events to become longer, open events to become shorter, low-activity gating modes to become more prevalent, or any combination of the above mechanisms. Of importance, each of these mechanisms results in distinct kinetic signatures, which ultimately define how the modulator affects biological function (Popescu, 2005; Popescu et al., 2010).

To delineate how ifenprodil affects the gating mechanism of NMDA receptors, we examined single-channel currents produced by 2B-containing NMDA receptors in the presence of ifenprodil and in conditions that minimized confounding effects by ambient extracellular ligands. On the basis of these results, we conclude that ifenprodil-binding causes channel closures to become longer, and thus openings to become less frequent by increasing an energetic barrier to channel activation; it also causes openings to become on average shorter by favoring low open probability gating modes. These results reveal an intrinsic effect of ifenprodil on channel gating and represent an important element in anticipating how ifenprodil affects NMDA receptor responses in situ.

Materials and Methods

All methods were similar to those described in detail previously (Kussius et al., 2009; Amico-Ruvio and Popescu, 2010). In brief, rat GluN1-1a (NR1-1a, U08261) and GluN2B (NR2B, NM012574) clones were expressed from pcDNA3.1(+) in human embryonic kidney 293 cells together with GFP.

Whole-cell currents were recorded with intracellular solution containing 135 mM CsF, 33 mM CsOH, 2 mM $MgCl_2$, 1 mM $CaCl_2$, 10 mM HEPBS, and 11 mM EGTA, pH 7.4 (CsOH) and were clamped at −70 mV. Clamped cells were perfused with extracellular solution containing 150 mM NaCl, 2.5 mM KCl, 0.5 mM $CaCl_2$, 10 mM HEPES, 0.01 mM EDTA, and 0.1 mM glycine, with 1 mM glutamate and 150 nM ifenprodil added as specified. Currents were amplified and low pass-filtered at 2 kHz (Axopatch 200B; four-pole Bessel), sampled at 5 kHz (Digidata, 1322A), and written into digital files with pClamp 10 (Molecular Devices, Sunnyvale, CA). Analyses were done with OriginPro 8.0 software.

Excised patch currents were recorded with pipette (intracellular) solution containing 135 mM CsF, 33 mM CsOH, 2 mM $MgCl_2$, 1 mM $CaCl_2$, 10 mM HEPES and 11 mM EGTA, adjusted to pH 7.4 (CsOH) and clamped at −70 mV. Upon reaching the outside-out configuration the patch was perfused with (extracellular) solution containing 150 mM NaCl, 2.5 mM KCl, 0.5 mM $CaCl_2$, 0.1 mM glycine, 0.01 mM EDTA, and 10 mM HEPBS, adjusted to pH 8.0 with NaOH. Glutamate (1 mM) and/or ifenprodil (150 nM) was added as indicated. Two extracellular solutions were applied simultaneously through a glass theta tube (2.0 mm diameter; Harvard Apparatus Inc., Holliston, MA). A lightly pressurized perfusion system maintained the flow rate at 200 μl/min and helped to form a sharp interface between the two streams. The recording pipette containing the excised membrane patch was positioned within one stream close to the interface, and the theta tube was mounted on a piezoelectric translator (Burleigh LSS-3100/3200) and used to exchange solution around the patch pipette. Open-tip potential measurements done at the end of each experiment showed that the 10 to 90% exchange occurred within 0.15 to 0.25 ms (Amico-Ruvio et al., 2011). Each barrel of the theta tube was connected to several solutions through a micro-manifold controlled with pinch valves (VC 6; Warner Instruments, Hamden, CT). Recorded currents were low pass-filtered at 5 kHz (Axopatch 200B; four-pole Bessel), sampled at 50 kHz (Digidata, 1440A), and written into digital files with pClamp 10.2 software. Traces were analyzed in Clampfit 10.2 and further with OriginPro 8.

Single-channel currents were recorded from cell-attached patches with glass electrodes filled with extracellular solution containing 150 mM NaCl, 2.5 mM KCl, 1 mM EDTA, 10 mM HEPBS, 1 mM glutamate, and 0.1 mM glycine, adjusted to pH 8.0 with NaOH. Channel openings were recorded as sodium influxes after applying +100 mV through the recording pipette. Currents were amplified and low pass-filtered at 10 kHz (Axopatch 200B; four-pole Bessel), sampled at 20 kHz (PCI-6229, M Series card; National Instruments, Austin, TX), and written into digital files with QuB acquisition software (http://www.qub.buffalo.edu, University at Buffalo, Buffalo, NY).

Processing and analyses were done on records that were selected to have only one active channel and required minimum processing, as described in detail previously (Kussius et al., 2009). Idealization (SKM) and modeling (MIL) were done in QuB using 12-kHz digitally filtered data, onto which we subsequently imposed a 0.15-ms resolution. Values for time constants, component areas, and rate constants were calculated with the models indicated. Calculated values along with all other kinetic parameters measured were tabulated and reported as means ± S.E.M. Significance of differences was evaluated with two-tailed Student's t tests assuming equal variance, were considered significant for $p < 0.05$, and were expressed as fold-change = (experimental/control) or as percent change = [(experimental/control) − 1] × 100.

Free-energy profiles were constructed using the rate constants in each model and the relationship $\Delta\Delta G_0 = -k_B T \ln K_{eq}$, where k_B is the

Boltzmann constant, T is the absolute temperature, and K_{eq} is the equilibrium constant of the transition considered. Barrier heights were of arbitrary magnitude and are represented as $E_n = \Delta G^0_n + k_B T(10 - \ln k_{+n})$.

Ensemble responses to square jumps into 1 mM glutamate were simulated as the sum of time-dependent open-state occupancies and were analyzed in a manner similar to that for experimental macroscopic traces (Popescu et al., 2004). We used previously reported microscopic rates for glutamate binding and dissociation: $k_+ = 6 \times 10^6$ M^{-1} s^{-1} and $k_- = 15$ s^{-1}, respectively (Amico-Ruvio and Popescu, 2010).

Results

Single-Channel Kinetics of Ifenprodil-Bound 2B Receptors. Ifenprodil concentrations reduce NMDA receptor responses in a biphasic manner and the high-affinity component is specific to 2B-containing NMDA receptors (Carter et al., 1988; Reynolds and Miller, 1989; Legendre and Westbrook, 1991). At physiological pH, the reported half-maximal inhibition for this high-affinity component is in the 130 to 340 nM range (Williams, 1993; Kew et al., 1996; Pahk and Williams, 1997; Mott et al., 1998; Perin-Dureau et al., 2002). We focused on the mechanism of high-affinity inhibition by recording single-channel activity from one-channel cell-attached patches of human embryonic kidney 293 cells transiently transfected with GluN1-1a and GluN2B subunits in the presence of 150 nM ifenprodil (IFN) (Fig. 1A). To limit the effects of contemporaneous extracellular ligands, we recorded single-channel activity in the presence of maximally effective concentrations of glutamate and glycine (1 and 0.1 mM, respectively; each >100-fold EC_{50}), we included a strong metal chelator in the recording pipette to remove trace divalent cations (1 mM EDTA), and we clamped proton concentrations at 10 nM (pH 8) with a buffer that is highly effective in this concentration range (10 mM HEPBS, $pK_a = 8.3$). As controls, we used a set of recordings obtained in identical conditions and the absence of ifenprodil (CTR) (Fig. 1B) (Amico-Ruvio and Popescu, 2010). Both data sets included only records that originated from a single active channel, and we processed and analyzed all records in an identical manner (Kussius et al., 2009; Amico-Ruvio and Popescu, 2010).

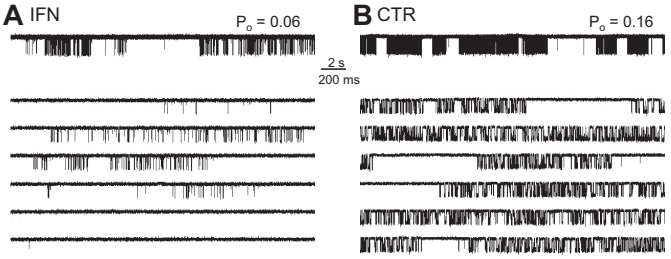

Fig. 1. Effects of ifenprodil on single 2B receptors. Traces represent steady-state inward sodium fluxes recorded from cell-attached patches that contained in the recording pipette one active 2B channel. A, with ifenprodil (IFN, 150 nM). B, without ifenprodil (CTR). For each condition, a 50-s segment is illustrated at two time resolutions in the top and middle panels, respectively; the bottom panels expand the underlined segment and is displayed filtered, as for analyses, at 12 kHz. All traces represent inward Na^+ currents as downward deflections from a zero-current baseline; P_o indicates the open probability calculated for the entire parent record.

We found that ifenprodil decreased the average equilibrium open probability (P_o) of 2B receptors ~4-fold with no change in the single-channel amplitude ($p > 0.05$) (Table 1). Thus, the ifenprodil concentration selected (150 nM) was sufficient to produce a substantial effect on channel gating and had no effect on single-channel conductance. Furthermore, we were able to attribute the decrease in P_o to a ~2-fold increase in the mean duration of closures (MCT) and a ~1.6-fold decrease in mean duration of openings (MOT) (Table 1). These results are consistent with previous reports of ifenprodil effects on single-channel activity of neuronal NMDA receptors (Legendre and Westbrook, 1991). Next, we examined in closer detail the mechanism by which these gating effects arose.

Ifenprodil-Bound Receptors Had Longer Closures and More Short Openings. The NMDA receptor gating mechanism of 2B receptors, although complex, has been well characterized (Banke and Traynelis, 2003; Erreger et al., 2005; Amico-Ruvio and Popescu, 2010). In the conditions used in this study, the steady-state gating reaction consists of frequent transitions between five closed and two open states and occasional gating-mode shifts (Amico-Ruvio and Popescu, 2010). Three modes, with low, medium, and high open probabilities, differ primarily in the duration of the longer of two joined open states, and each mode can last from several seconds to several minutes (Popescu and Auerbach, 2003; Popescu, 2012). Thus, our result that ifenprodil decreased channel P_o by increasing MCT and decreasing MOT could reflect two distinct underlying mechanisms. In one, ifenprodil-bound and ifenprodil-free receptors populate the same kinetic states but distribute with different probabilities across states. Alternatively, the gating sequence itself is altered: receptors access new modulator-induced closed (e.g., blocked) states, and some open states may become inaccessible. To investigate the underlying mechanism we examined the distribution of closed and open durations present in our single-channel records.

All the one-channel records we obtained with IFN ($n = 6$) were well described with five closed components (E_1–E_5), as we had reported previously for CTR ($n = 31$) (Fig. 2A) (Amico-Ruvio and Popescu, 2010). This result indicates that ifenprodil binding did not produce additional closed conformations; instead it altered specific closed components: E_2, E_3, and E_4 were ~3-fold longer, and the area corresponding to the E_2 component increased 1.6-fold (from 19 ± 2 to 31 ± 3%, $p < 0.05$), at the expense of a 3-fold decrease in the E_1 component area (from 20 ± 2 to 6.8 ± 0.4%, $p < 0.05$) (Fig. 2B). Of importance, ifenprodil did not change the time constant of the longest closed component (E_5), which encompasses the longest desensitized events. Together with the observation that ifenprodil did not alter channel conductance, these results strongly exclude contributions by channel block and longer dwells in desensitized conformations as elements of the inhibitory mechanism of ifenprodil.

A similar analysis of open periods is more difficult to perform and to interpret because of the heterogeneity introduced by modal behavior (Popescu, 2012). In practice, depending in part on the length of the observed period, any record obtained from control 2B receptors may or may not capture modal transitions. Thus, any record can have two, three, or four

open components, corresponding to one, two, or three gating modalities present (Popescu and Auerbach, 2003; Amico-Ruvio and Popescu, 2010). Ifenprodil-treated channels maintained this heterogeneity in the number of open components, indicating that modal behavior is preserved in the presence of ifenprodil. Half of the IFN records had three components (τ_{fast}, τ_{low}, and τ_{med}), indicative of low and medium gating modes, and the remainder had four open components (τ_{fast}, τ_{low}, τ_{med}, and τ_{high}), indicative of all three gating modes. Figure 3A illustrates open event distributions obtained for two files, CTR and IFN, each having the maximum number of open components.

Ifenprodil Favored Gating in Low Open Probability Modes. To our surprise, when we compared time constants of the open components in the two data sets, except for a small decrease in τ_{low} (from 2.7 ± 0.1 to 2.2 ± 0.2 ms, $p < 0.05$), we found no other statistically significant difference ($p > 0.05$, Student's t test). On the basis of this observation, we reasoned that the shorter MOT observed in the ifenprodil-treated set must reflect a larger proportion of modes with shorter openings (Table 2). This inference was supported by significantly smaller areas observed in the IFN data set for the medium and high components (a_{med} and a_{high}) (Fig. 3B). To test whether this result may have been skewed by the substantially fewer records we obtained with ifenprodil relative to CTR, we selected from each set those records that displayed all four open components (CTR, $n = 6$ and IFN, $n = 3$). Similar to our results obtained for the complete data sets, the ifenprodil-treated group had significantly shorter MOT (1.4-fold, $p < 0.006$), had essentially unchanged time constants for the four open components ($p > 0.05$), and had considerably higher proportion of short components (a_{fast} and a_{low}) (Table 2). On the basis of these analyses, we conclude that ifenprodil-bound receptors had shorter openings on average because they spent more time in the low-activity gating mode; however, medium- and high-activity modes were still accessible and during these periods, openings were of a duration similar to those of ifenprodil-free receptors. This inhibitory mechanism was unexpected because it was not observed with zinc, which is also an NTD ligand (Amico-Ruvio et al., 2011).

Kinetic Models of Ifenprodil Actions on 2B Receptors. Next, we summarized these kinetic changes using a 5C1O kinetic scheme, which, although clearly a simplification of the complex rearrangements that occur during NMDA receptor gating, captures the salient features of its microscopic and macroscopic behaviors (Popescu et al., 2004; Kussius et al., 2009). Because, in this study, we used high concentrations of glutamate and glycine (1 and 0.1 mM, respectively, which are >100-fold EC_{50}), the agonist dissociation events were briefer than the time resolution used in our analyses, and, thus, we were safe to assume that all events recorded reflected dwells in agonist-bound receptor states. Despite these simplifying assumptions, the kinetic modeling analysis provided important mechanistic insight as presented below.

Given that our stationary recordings were done using only half of the maximally effective IFN concentration (150 nM), we expected that in our IFN data set each record contained events corresponding to dwells in IFN-free as well as in IFN-bound states. This condition can be conceptualized with two types of models. Fitting the data by a 5C1O model, which represents the average behavior of IFN-bound and IFN-free receptor at the concentration used, identifies IFN-dependent transitions and provides insight into mechanism. Fitting the data by a tiered model, in which each arm represents IFN-free and IFN-bound gating reactions, can provide insight into ifenprodil binding kinetics and mechanism.

According to the average 5C1O model, 150 nM ifenprodil changed only a subset of the 10 rate constants considered: $k_{3\to2}$, $k_{2\to3}$, $k_{4\to2}$, and $k_{1\to O}$ (Fig. 4A). Each of these four rate constants decreased to a similar extent (3- to 4-fold) and resulted in significant changes in only two equilibria: K_{2-4} (from 0.3 to 0.8) and K_{1-O} (from 4.6 to 1.6). On the basis of this mechanisms, the decrease in open-state occupancy at equilibrium is compensated for mainly by a ~2.5-fold increase in the occupancy of the desensitized state C_4 (Fig. 4B). We next used the deduced CTR and IFN reaction mechanisms to calculate the relative free-energy fluctuations during gating, and we illustrate these in Fig. 4C. To compare the two profiles, we arbitrarily aligned these at the free-energy level of the first fully liganded closed state C_3. According to this interpretation, ifenprodil decreased receptor activity by increasing the activation barrier to the first gating step. In addition, this analysis illustrates changes in the stability of open states, which, based on the results presented in the previous section, most likely reflects a preference of IFN-bound receptors for gating in the low-activity mode. Thus, based on these results, we suggest that ifenprodil inhibits 2B receptors by raising the activation barrier to the first gating transition and by favoring gating in low P_o modes.

A more accurate representation of channel gating in the subsaturating ifenprodil concentration used in this study can be achieved with models that incorporate explicit IFN-free and IFN-bound states. This analysis may also provide insight into the kinetics and mechanisms of ifenprodil binding. To accomplish this, we considered a tiered model that contained separate gating arms for IFN-free and IFN-bound receptors. In the IFN-free arm, all rate constants were fixed to values measured in the absence of ifenprodil (Figs. 4A and 5, CTR), and in the IFN-bound arm, the rate constants that were found invariant in the IFN data set relative to the CTR data set were fixed to IFN values (Figs. 4A and 5, IFN: $k_{2\to1}$, $k_{1\to2}$, $k_{2\to4}$, $k_{3\to5}$, and $k_{5\to3}$); all other rate constants in the IFN-bound arm were allowed to vary during fitting: $k_{3\to2}$, $k_{2\to3}$, $k_{4\to2}$, $k_{1\to O}$, and $k_{O\to1}$. Initially, we connected the two arms

TABLE 1
Effects of ifenprodil on average kinetic properties of individual 2B receptors

	Amplitude	P_o	MCT	MOT	n	Duration	Events
	pA		*ms*			*min*	*×10⁶*
CTR	10.0 ± 0.3	0.20 ± 0.03	37 ± 6	5.1 ± 0.4	31	904	4.1
IFN	9.6 ± 0.5	0.05 ± 0.01*	82 ± 20*	3.2 ± 0.2*	6	213	0.4
% change		−75%	+122%	−37%			

*$p < 0.05$ (Student's t test).

with ifenprodil association/dissociation transitions and allowed these to vary during fitting, but this model failed to represent the IFN data set, even when binding and dissociation rates were constrained to be equal regardless of the position in the model. Next, we considered models in which ifenprodil binding/dissociation transitions were allowed only between a subset of gating steps. Consistently, the model represented in Fig. 5 returned best fitting scores using a log likelihood criterion. This is an interesting result because it implies that transitions between IFN-free and IFN-bound states occur with the highest probability when the receptor resides in the closed state C_3. Given that the C_3 state represents a collection of closed receptor conformations, which at a minimum includes brief agonist-free states, agonist-bound states with open and closed agonist-binding clefts, and agonist bound states that differ in the relative position of the ligand-binding domains, this analysis may indicate that ifenprodil binds to NMDA receptors before or immediately after glutamate binding. However, the implication of state-dependent binding requires more detailed investigation.

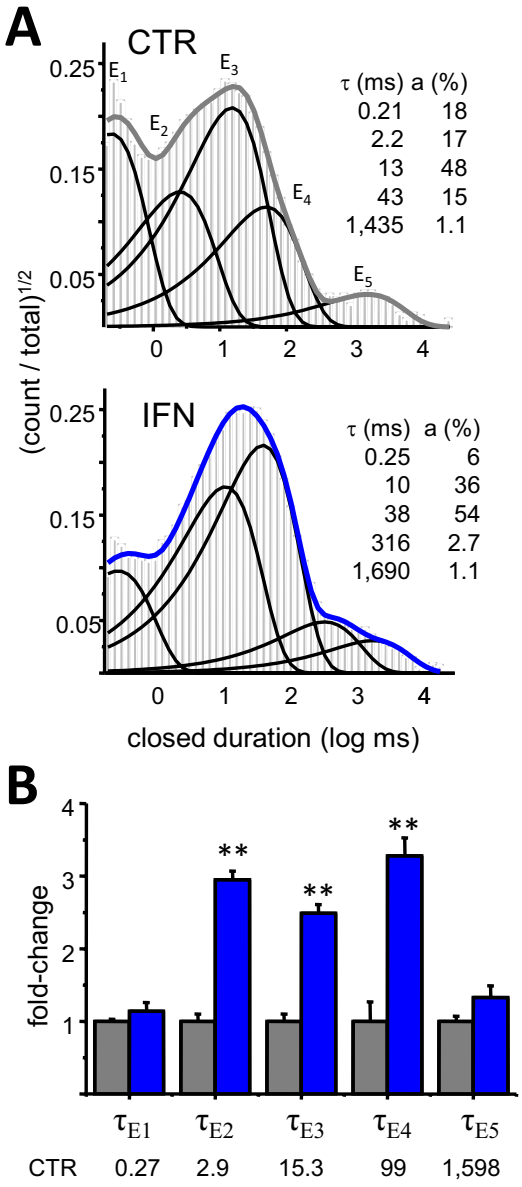

Fig. 2. Ifenprodil prolongs specific closed components. A, closed intervals observed in two records obtained from 2B receptors in the absence (CTR, 42,360 events) and presence of ifenprodil (IFN, 150 nM, 78,017 events). Probability density functions (thick lines) were calculated by fitting kinetic 5C4O state models to the displayed data; thin lines represent individual exponential components. Their time constants (τ, milliseconds) and areas (a, percentages) are given as insets. B, summary of closed time constants in the two conditions [CTR (gray), $n = 31$; IFN (blue), $n = 6$]. Average values for CTR are given in milliseconds below each component. **, $p < 0.003$ (Student's t test).

Of importance, the tiered model estimated values for the ifenprodil association and dissociation rate constants: $k_{on} = 1.4 \times 10^9\ M^{-1}\ s^{-1}$ and $k_{off} = 90\ s^{-1}$ ($K_d = 64$ nM). The association rate constant estimated here is 20-fold faster than that previously estimated as a blocking rate constant in hippocampal neurons ($6 \times 10^7\ M^{-1}\ s^{-1}$) (Legendre and Westbrook, 1991), and the estimated K_d is 5-fold lower than that determined from calorimetric measurements for a mixture of soluble N-terminal domains detached from N1 and N2B subunits ($K_d = 320$ nM) (Karakas et al., 2011). However, our K_d matches closely the IC_{50} determined in *Xenopus* oocytes with the two-electrode voltage-clamp method ($IC_{50} = 100$ nM) (Karakas et al., 2011).

Experimental Validation for the Proposed Mechanism of Ifenprodil Action. The models illustrated in Fig. 4A postulate a mechanism for ifenprodil inhibition in which a shift in the equilibrium distribution of 2B receptors away from open states is compensated for by a ~2.5-fold increase in the occupancy of the desensitized state C_4 (Fig. 4B). However, because the C_4 state is only scarcely populated (~5% in the absence of ifenprodil), the model predicts that this change will not visibly affect the time course of macroscopic desensitization, as illustrated by simulations with CTR and IFN models (Fig. 6A). We tested this prediction by recording whole-cell currents after long (5-s) applications of glutamate (1 mM) while glycine was continuously present (0.1 mM). Results showed that indeed, relaxation to equilibrium occurred with a similar time course whether ifenprodil was present or not ($n = 6$ cells for each condition) (Fig. 6A). In addition, we observed that the inhibition produced by 150 nM ifenprodil was less pronounced for whole-cell current responses (~50%) than that observed for cell-attached receptors (75%) (Fig. 6A; Table 1). This may reflect a higher incidence of receptors already gating in low-activity mode in this preparation.

Further, we used the deduced models from Fig. 4A to anticipate how ambient ifenprodil (150 nM) may affect synaptic NMDA receptor responses. Simulation results suggested that the major effect of ifenprodil will be a substantial decrease in charge transfer (~3.5-fold) due primarily to a comparable decrease in current amplitude and only small change in deactivation time course. To test this prediction, we recorded currents from 2B receptors residing in excised outside-out patches and exposed to brief (10 ms) pulses of glutamate (1 mM) in continuous glycine (0.1 mM). As predicted by our model, IFN caused a substantial decrease in current amplitude and only subtle changes in deactivation kinetics (Fig. 6B). The close match between the kinetic behaviors of macroscopic traces predicted by our model and that of responses recorded from whole-cell and excised-patch preparations represent a strong argument that the kinetic mechanism deduced from single-channel data captures the relevant features of the ifenprodil effects on 2B-containing NMDA receptors.

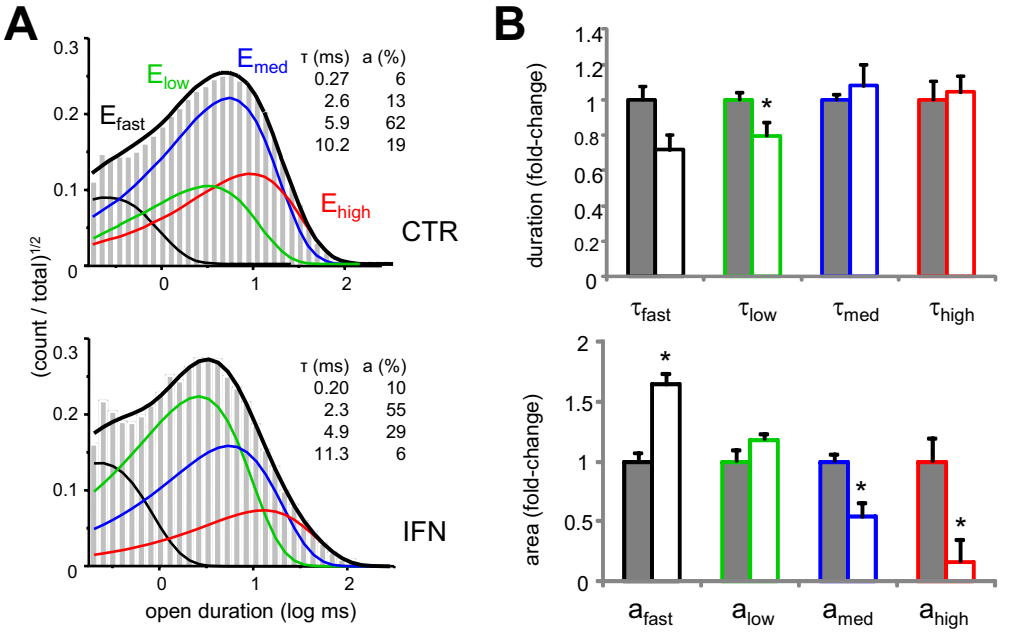

Fig. 3. Ifenprodil favors low-activity mode gating of 2B receptors. A, open durations observed in two records obtained from 2B receptors in the absence (CTR, 82,224 events) (top) and presence of ifenprodil (IFN, 150 nM, 78,017 events) (bottom). Thick lines represent probability density functions calculated from fits to 5C4O state models; thin lines represent individual exponential components. Insets, time constants (τ, milliseconds) and areas (a, percentages) for the respective record. B, summary of changes for open event distributions. CTR, gray; IFN, white. *, $p < 0.05$ (Student's t test).

Discussion

In this report, we describe the effects of subsaturating concentrations of ifenprodil on currents recorded from 2B NMDA receptors. We recorded on-cell single-molecule activity in the presence of maximally effective concentrations of agonists and in the virtual absence of extracellular modulators. Relative to controls, ifenprodil (150 nM) reduced channel P_o by 75% largely because in its presence a set of channel closures were longer and because the fraction of short openings was larger. Within the context of a multistep gating reaction, these observations were consistent with a mechanism in which ifenprodil-bound receptors gated according to the same sequence of activation, desensitization, and mode switching transitions experienced by ifenprodil-free receptors, with only a subset of rate constants changed. The reduced activity could be explained by a mechanism for which ifenprodil binding increased the energy barrier to activation and favored gating in the low-activity mode. In addition, the proposed mechanism estimates association and dissociation rate constants for ifenprodil.

This mechanism predicted that macroscopic responses elicited by glutamate in the presence of ifenprodil would have lower peak amplitudes and would have similar deactivation and desensitization profiles and the degree of inhibition will be greater for preparations containing receptors that gate preferentially in high and/or medium modes. We were able to gather preliminary experimental support for these predictions. We recorded macroscopic responses to long (5-s) and brief (10-ms) applications of glutamate (1 mM) and observed that, indeed, responses recorded when ifenprodil was present had lower amplitudes but largely similar deactivation and desensitization time courses relative to same-cell controls. These results strongly indicate that our model incorporates the salient features of the ifenprodil inhibitory mechanism. In a previous study we showed that the biphasic nature of NMDA receptor deactivation reflects two NMDA receptor populations gating in distinct modes (Zhang et al., 2008). Thus, a modulator capable of altering receptor distribution across modes will certainly influence deactivation kinetics and the time course of synaptic currents. However, because of the low incidence of modal changes in our stationary recordings, we were not able to model either kinetics within specific modes nor the kinetics of mode switching; thus, here we only examined the overall profile of the current decay. Still, both the simulated and the recorded responses clearly showed that ifenprodil changed the time course of 2B receptor deactivation; however, these changes were much smaller than the dramatic decrease in current amplitude, and, thus, the major effect on the magnitude of charge transfer was accounted for by changes in current amplitude.

The degree of inhibition for whole-cell currents (50%) was lower than that for excised-patch currents and also lower than predicted from cell-attached measurements (75%). This decrease in inhibitory effect for preparations in which the integrity of the cellular membrane is compromised (whole-cell and excised-patch) may reflect an increased prevalence in these conditions of low-activity modes, which are inhibited to a lesser degree than high-activity modes. Legendre and

TABLE 2
Effects of ifenprodil on individual open components

	MOT	τ_{fast}	a_{fast}	τ_{low}	a_{low}	τ_{med}	a_{med}	τ_{high}	a_{high}
	ms		%	*ms*	%	*ms*	%	*ms*	%
CTR ($n = 6$)	5.0 ± 0.3	0.25 ± 0.02	6 ± 1	2.7 ± 0.3	24 ± 4	5.7 ± 0.4	63 ± 2	16 ± 3	6 ± 3
IFN ($n = 3$)	3.5 ± 0.2*	0.21 ± 0.01	11 ± 1*	2.2 ± 0.1	52 ± 2*	5.4 ± 0.3	32 ± 3*	14 ± 1	4 ± 1
% change	−30%		+83%		+117%		−49%		

*$P < 0.02$ (Student's t test).

Westbrook (1991) also noted that ifenprodil inhibition was less pronounced for whole-cell than for excised-patch currents and that whole-cell current inhibition is further attenuated after channels undergo calcium-dependent inactivation (Legendre and Westbrook, 1991). However, our experiments did not address these issues.

The uncertainty of mode switching notwithstanding, our results demonstrate that ifenprodil reshuffled receptors across the spectrum of available conformations. As expected for an inhibitor, ifenprodil decreased the relative occupancy of open relative to closed states. In addition, our results indicated that rather than uniformly increasing the occupancies of all closed states, ifenprodil changed the relative distribution across closed states as well. This result may be the basis for the additional functional effects of ifenprodil on NMDA receptors. Ample literature reports document that ifenprodil binding to NMDA receptors enhances the inhibitory effects of other NTD ligands such as protons and zinc and interferes with polyamine potentiation (Reynolds and Miller, 1989; Ransom, 1991; Mott et al., 1998; Rachline et al., 2005). In addition, ifenprodil affects the potency of LBD ligands glycine, glutamate, and NMDA (Ransom, 1991; Kew et al., 1996; Mott et al., 1998). For these reasons, it has been proposed that rather than having an intrinsic action on receptor open probability, ifenprodil acts by enhancing the inhibitory potency of coincident ligands and/or causes agonists to become less effective (Ransom, 1991; Mott et al., 1998).

We proposed previously that allosteric modulators, those ligands that cause a redistribution of NMDA receptors across accessible states, in conjunction with changing P_o, can also change other receptor functionalities such as their apparent sensitivity to coincident ligands (Popescu, 2005). Such a combined effect would be observed if a given modulator changed the proportion of open states and also the proportion of states that have distinct affinities for separate ligands, whether these have distinct conductances or not. The results presented here show that 150 nM ifenprodil caused ~75% inhibition of 2B receptor currents even when receptors were fully bound with glutamate and glycine, in the absence of trace amounts of Ca^{2+} and Zn^{2+} and with protons at 10-fold lower than the half-effective inhibitory dose (Traynelis and Cull-

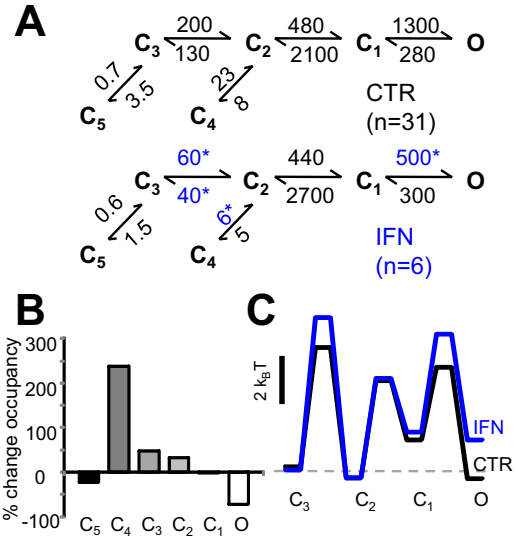

Fig. 4. Kinetic mechanism of ifenprodil inhibition. A, reaction mechanisms for ifenprodil-free (CTR) and ifenprodil-bound 2B receptors (IFN); rate constants for the steps explicitly incorporated in the model were estimated from fits to one-channel records and are given in seconds^{-1} as averages for the records in each data set. *, $p < 0.05$ (Student's t test). All states represent receptor conformations fully bound with glutamate and glycine. C, nonconductive; O, conductive. B, state-occupancy changes calculated from the reaction mechanisms in A. C, relative free-energy fluctuations during gating were calculated with the rate constants in A. Desensitized states (C_4 and C_5) are omitted for simplicity; profiles are arbitrarily aligned at C_3.

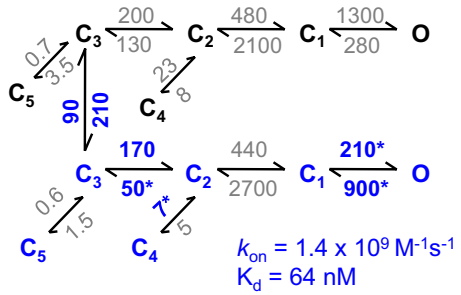

Fig. 5. Ifenprodil binding kinetics tiered model represents the gating mechanisms of ifenprodil-free (upper arm) and ifenprodil-bound (lower arm) receptors; transitions between arms are allowed only between the C_3 states. The model was fit to data obtained in 150 nm ifenprodil ($n = 3$): rate constants in gray were fixed to the values obtained for CTR and IFN conditions in Fig. 4A, whereas the rates in blue were allowed to vary. Values for each transition represent the average of the rates estimated for each file and are given in seconds^{-1}. The calculated association rate constant (k_{on}) and the equilibrium dissociation constant (K_d) for ifenprodil are indicated.

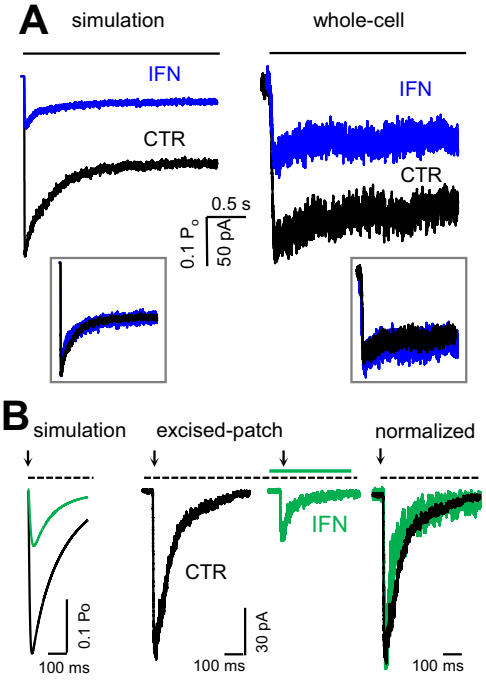

Fig. 6. Ifenprodil effects on 2B macroscopic responses. A, macroscopic responses to a long (5-s) pulse of 1 mM Glu (black line) were simulated with the models in Fig. 4A, to which glutamate binding steps were appended as described under *Materials and Methods* (left) and were recorded as whole-cell currents in the absence (black) or presence (blue) of 150 nM ambient ifenprodil (right); insets show the same traces normalized to peaks. B, macroscopic responses to a brief (10-ms) pulse of 1 mM Glu (black arrow) were simulated as above (left) and were recorded from outside-out patches in the absence (black) or presence (green) of 150 nM ambient ifenprodil (middle); recorded traces are normalized to peak and are overlaid for comparison (right).

Candy, 1990; Mott et al., 1998; Banke et al., 2005). Thus, our results support a mechanism for which ifenprodil binding has intrinsic consequences on channel gating, which by means of changing the proportion of states with high and low affinity for secondary ligands, can also change the receptor's sensitivity to these ligands.

Structural and functional evidence has consolidated the view that although separate, the molecular determinants of proton, zinc, and ifenprodil inhibition are located within the N-terminal layer. Our results indicate that the mechanism of ifenprodil inhibition is distinct from that of protons or zinc, the two NTD ligands for which kinetic models have been proposed to date. Therefore, our new observations substantiate the view that perturbations in the NTD, rather than deployment of a common inhibitory mechanism, exert specific actions, which may be exploited for separate clinical purposes.

In summary, our results add to the already ample evidence that NMDA receptors are highly allosteric molecules and provide mechanistic support for the hypothesis that the sum result of NMDA receptor activation is highly dependent on the composition of their extra- and intracellular environments. Keeping in mind that ifenprodil is investigated as a potential therapeutic agent for a number of NMDA receptor-mediated pathologies and is also widely used as a research tool, it will be important to consider its action in context with coexisting factors. As quantitative descriptions of allosteric perturbations, either chemical or genetic, become available, it will be possible to predict receptor behaviors in highly customized environments. Our report represents one necessary element toward the greater goal of anticipating receptor drug effects in specific conditions, thus, forecasting potential outcomes with greater confidence and accuracy.

Acknowledgments

We thank Eileen M. Kasperek for assistance with molecular biology and cell culture.

Authorship Contributions

Participated in research design: Amico-Ruvio, Paganelli, and Popescu.

Conducted experiments: Amico-Ruvio, Paganelli, and Myers.

Performed data analysis: Amico-Ruvio, Paganelli, and Popescu.

Wrote or contributed to the writing of the manuscript: Amico-Ruvio, Paganelli, and Popescu.

References

Amico-Ruvio SA and Popescu GK (2010) Stationary gating of GluN1/GluN2B receptors in intact membrane patches. *Biophys J* **98:**1160–1169.

Amico-Ruvio SA, Murthy SE, Smith TP, and Popescu GK (2011) Zinc effects on NMDA receptor gating kinetics. *Biophys J* **100:**1910–1918.

Banke TG, Dravid SM, and Traynelis SF (2005) Protons trap NR1/NR2B NMDA receptors in a nonconducting state. *J Neurosci* **25:**42–51.

Banke TG and Traynelis SF (2003) Activation of NR1/NR2B NMDA receptors. *Nat Neurosci* **6:**144–152.

Carron C, Jullien A, and Bucher B (1971) Synthesis and pharmacological properties of a series of 2-piperidino alkanol derivatives. *Arzneimittelforschung* **21:**1992–1998.

Carter C, Benavides J, Legendre P, Vincent JD, Noel F, Thuret F, Lloyd KG, Arbilla S, Zivkovic B, and MacKenzie ET (1988) Ifenprodil and SL 82.0715 as cerebral anti-ischemic agents. II. Evidence for *N*-methyl-D-aspartate receptor antagonist properties. *J Pharmacol Exp Ther* **247:**1222–1232.

Cull-Candy SG (2007) NMDA receptors, in *Encyclopedia of Life Sciences,* John Wiley & Sons, London.

Erreger K, Dravid SM, Banke TG, Wyllie DJ, and Traynelis SF (2005) Subunit-specific gating controls rat NR1/NR2A and NR1/NR2B NMDA channel kinetics and synaptic signalling profiles. *J Physiol* **563:**345–358.

Furukawa H and Gouaux E (2003) Mechanisms of activation, inhibition and specificity: crystal structures of the NMDA receptor NR1 ligand-binding core. *EMBO J* **22:**2873–2885.

Furukawa H, Singh SK, Mancusso R, and Gouaux E (2005) Subunit arrangement and function in NMDA receptors. *Nature* **438:**185–192.

Huggins DJ and Grant GH (2005) The function of the amino terminal domain in NMDA receptor modulation. *J Mol Graph Model* **23:**381–388.

Inanobe A, Furukawa H, and Gouaux E (2005) Mechanism of partial agonist action at the NR1 subunit of NMDA receptors. *Neuron* **47:**71–84.

Kalia LV, Kalia SK, and Salter MW (2008) NMDA receptors in clinical neurology: excitatory times ahead. *Lancet Neurol* **7:**742–755.

Karakas E, Simorowski N, and Furukawa H (2009) Structure of the zinc-bound amino-terminal domain of the NMDA receptor NR2B subunit. *EMBO J* **28:**3910–3920.

Karakas E, Simorowski N, and Furukawa H (2011) Subunit arrangement and phenylethanolamine binding in GluN1/GluN2B NMDA receptors. *Nature* **475:**249–253.

Kew JN, Trube G, and Kemp JA (1996) A novel mechanism of activity-dependent NMDA receptor antagonism describes the effect of ifenprodil in rat cultured cortical neurones. *J Physiol* **497 (Pt 3):**761–772.

Kussius CL, Kaur N, and Popescu GK (2009) Pregnanolone sulfate promotes desensitization of activated NMDA receptors. *J Neurosci* **29:**6819–6827.

Lee CH and Gouaux E (2011) Amino terminal domains of the NMDA receptor are organized as local heterodimers. *PLoS ONE* **6:**e19180.

Legendre P and Westbrook GL (1991) Ifenprodil blocks *N*-methyl-D-aspartate receptors by a two-component mechanism. *Mol Pharmacol* **40:**289–298.

Mott DD, Doherty JJ, Zhang S, Washburn MS, Fendley MJ, Lyuboslavsky P, Traynelis SF, and Dingledine R (1998) Phenylethanolamines inhibit NMDA receptors by enhancing proton inhibition. *Nat Neurosci* **1:**659–667.

Pahk AJ and Williams K (1997) Influence of extracellular pH on inhibition by ifenprodil at *N*-methyl-D-aspartate receptors in *Xenopus* oocytes. *Neurosci Lett* **225:**29–32.

Perin-Dureau F, Rachline J, Neyton J, and Paoletti P (2002) Mapping the binding site of the neuroprotectant ifenprodil on NMDA receptors. *J Neurosci* **22:**5955–5965.

Popescu G (2005) Principles of *N*-methyl-D-aspartate receptor allosteric modulation. *Mol Pharmacol* **68:**1148–1155.

Popescu G and Auerbach A (2003) Modal gating of NMDA receptors and the shape of their synaptic response. *Nat Neurosci* **6:**476–483.

Popescu G, Robert A, Howe JR, and Auerbach A (2004) Reaction mechanism determines NMDA receptor response to repetitive stimulation. *Nature* **430:**790–793.

Popescu GK (2012) Modes of glutamate receptor gating. *J Physiol* **590:**73–91.

Popescu GK, Murthy S, and Borschel WF (2010) Allosteric inhibitors of NMDA receptor functions: a next generation in CNS therapies. *Pharmaceuticals* **3:**3240.

Rachline J, Perin-Dureau F, Le Goff A, Neyton J, and Paoletti P (2005) The micromolar zinc-binding domain on the NMDA receptor subunit NR2B. *J Neurosci* **25:**308–317.

Ransom RW (1991) Polyamine and ifenprodil interactions with the NMDA receptor's glycine site. *Eur J Pharmacol* **208:**67–71.

Reynolds IJ and Miller RJ (1989) Ifenprodil is a novel type of *N*-methyl-D-aspartate receptor antagonist: interaction with polyamines. *Mol Pharmacol* **36:**758–765.

Sobolevsky AI, Rosconi MP, and Gouaux E (2009) X-ray structure, symmetry and mechanism of an AMPA-subtype glutamate receptor. *Nature* **462:**745–756.

Traynelis SF and Cull-Candy SG (1990) Proton inhibition of *N*-methyl-D-aspartate receptors in cerebellar neurons. *Nature* **345:**347–350.

Williams K (1993) Ifenprodil discriminates subtypes of the *N*-methyl-D-aspartate receptor: selectivity and mechanisms at recombinant heteromeric receptors. *Mol Pharmacol* **44:**851–859.

Zhang W, Howe JR, and Popescu GK (2008) Distinct gating modes determine the biphasic relaxation of NMDA receptor currents. *Nat Neurosci* **11:**1373–1375.

Address correspondence to: Dr. Gabriela K Popescu, University at Buffalo, Department of Biochemistry, 140 Farber Hall, 3435 Main St., Buffalo, NY 14214. E-mail: popescu@buffalo.edu